

Image Cover Sheet

CLASSIFICATION

SYSTEM NUMBER

8903

UNCLASSIFIED



TITLE

MEASUREMENT OF NOISE ON AN UNDERWATER TOWED BODY

System Number:

Patron Number:

Requester:

Notes:

DSIS Use only:

Deliver to: JR



0201 DREA
0202 403761
0203 6917

414 420

30a

30b vol 48
30c no 3 (pt 2)

Reprinted from THE JOURNAL OF THE ACOUSTICAL SOCIETY OF AMERICA, (Vol. 48, No. 3, (Part 2), 753-758, September 1970)

30 J 1970

Copyright, 1970, by the Acoustical Society of America

Printed in U. S. A.

30 E P 753-758

Received 17 November 1969

13.9, 13.7

04a

Measurement of Noise on an Underwater Towed Body

1101

1102

1103

R. Y. NISHI, J. H. STOCKHAUSEN, AND E. EVENSEN

0204a

Defence Research Establishment Atlantic, Defence Research Board of Canada, Dartmouth, Nova Scotia, Canada (CAN)

50

46 1970

0901 6
0902 13

Noise has been measured on a streamlined body of revolution towed by a hydrofoil craft at speeds up to 30 kt. The body was instrumented with accelerometers, flush-mounted hydrophones in the wall, and cylindrical hydrophones in the interior of the body. Towing was conducted with different lengths of cable. The noise in the body was found to result from body-wall vibrations, from farfield radiated noise sources, and from flow noise caused by pressure fluctuations in the turbulent boundary layer. Wall vibrations were found to be caused by cable vibrations, cavitation, and other flow-induced mechanisms. The pressure distribution along the towed body and thickness of the turbulent boundary layer have been calculated and are also presented to aid in the interpretation of the results.

INTRODUCTION

Towed bodies for acoustic measurements in the ocean have both oceanographic and military applications. At high towing speeds, flow noise produced by the motion of the body through the water can create a serious problem by degrading the data being collected. Flow noise is caused by pressure fluctuations in the turbulent boundary layer, by turbulence-excited wall vibrations, by eddies generated by surface roughness, and by eddies shed at tail fins. The last may be of particular importance as vibrations induced in the tail may also be transmitted to the body.

In the past, such diverse facilities as wind and water tunnels,¹⁻⁴ buoyancy-propelled bodies,^{5,6} bodies of revolution,⁷ and rotating cylinders^{1,8} have been used to measure the fluctuating wall pressure beneath the turbulent boundary layer. The available data from these various sources are in reasonable agreement, and the spectral and statistical properties of the fluctuating pressure field are becoming well-known.⁹ No similar work has been reported on towed bodies. Theoretical treatments exist for flow-excited vibrations, but most of these are concerned with specific models, for instance, simply supported rectangular flat plates.¹⁰

In addition to flow noise, noise in a towed body can be caused by sources associated with the towing process. Vibrations originating at the towing craft and towing-cable vibrations may be transmitted down the cable to the body and cause the walls to vibrate. If the body is towed at shallow depths, cavitation at local roughnesses and at appendages such as the tow point can

occur. Finally, the towing craft's radiated noise can produce noise at the towed body.

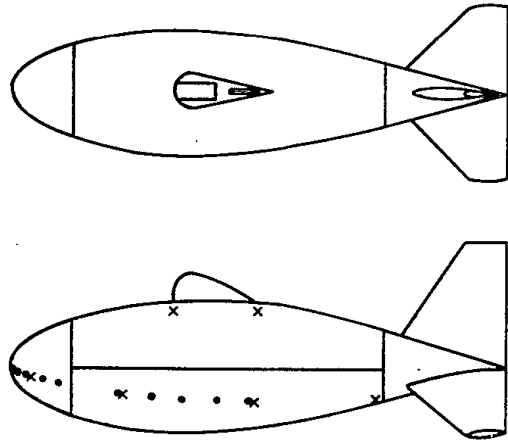
This paper describes noise measurements on a streamlined body of revolution towed at speeds up to 30 kt. The towed body, its instrumentation, the experimental conditions, and the hydrodynamic characteristics of the body are described and the results of the measurements presented to show the various noise mechanisms possible in the towed body.

I. EXPERIMENTAL

The towed body used in this investigation is a body of revolution based on an airfoil profile (NACA 64A025). The body, which is 6 ft long and 1½ ft at its maximum diameter, is stabilized by a triform fin arrangement with a vertical fin and two lower fins each set at 37° below the horizontal (Fig. 1). The shell is made of fiberglass of nominal thickness (¼ in.) and consists of three sections—nose cone, center section, and tail cone. The center section is reinforced by 11 equally spaced ribs. The upper-center section is removable in order to give access to the instrumentation, and the joint, when closed, is filled with paraffin wax. Joints in the lower half are permanently filled with epoxy resin. A pivoted tow staff with a fairing provided to reduce vortex shedding and cavitation is located at the top of the body (Fig. 2). The body is free flooding, ballasted with lead, and the total weight is 500 lb in air and 375 lb in water.

The body was instrumented with miniature flush-mounted hydrophones in the skin. The location of

DC



H/P No. 1 3 4 5 6 7 8 9 10

FIG. 1. Plan and profile of towed body showing locations of flush-mounted hydrophones and accelerometers. Body length—6 ft; max diameter—1.5 ft; ●—flush-mounted hydrophones, x—accelerometers.

these hydrophones (Atlantic Research LD-80), which have a sensitive diameter of 0.07 in.,¹¹ are shown in Fig. 1. The sensitivity of these hydrophones was measured *in situ*. In addition, end-capped lead-zirconate-titanate cylindrical hydrophones of ½-in. diam were installed inside the body in the nose section and just aft of the tow point. Several accelerometers (Brüel & Kjær type 4333) were also mounted on different parts of the body.

The various towing speeds and cable lengths used and the depths achieved are shown in Table I. In all cases runs were 2–3 min in duration, sufficiently long to provide a convenient check on the stationarity of the measured signal. The towing vessel, *BADDECK*, is a hydrofoil craft equipped with a cable winch and saddle for the towed body (Fig. 3) and becomes fully foil-borne at 25 kt. The tow cable used was a ¾-in.-diam steel cable with an inner core of seven conductors and sheathed in a sectional fairing to reduce drag and cable vibrations.

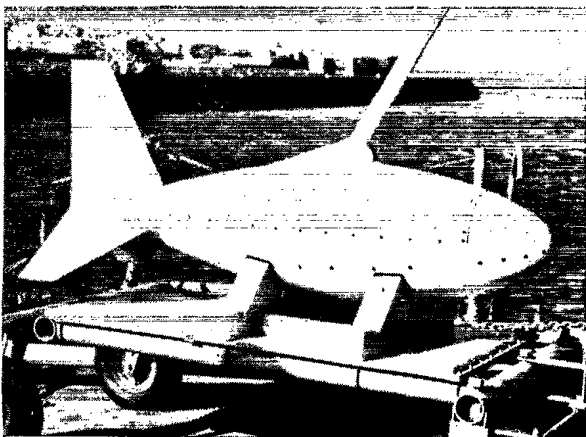


FIG. 2. Towed body showing tow-staff fairing and cable.

Four of the seven electrical conductors in the cable were used for signal transmission and the remaining three for power supply and switching control. A water-tight box in the body contained preamplifiers, amplifiers, and switching circuits controlled from the towing vessel. The signals were further amplified on the towing vessel and recorded on magnetic tape. Analysis of the data was later performed in ⅓-oct bands from 50 Hz to 20 kHz.

II. HYDRODYNAMIC CHARACTERISTICS OF BODY

A proper evaluation of flow noise caused by boundary-layer-pressure fluctuations requires a knowledge of the thickness of the turbulent boundary layer and the location on the body of the transition point from laminar to turbulent flow. Since a direct measurement of the extent of the boundary layer was not possible, the transition point and the thickness of the boundary layer were calculated from theoretical considerations. Normally, flat-plate approximations are used in estimating the thickness of the boundary layer. Because pressure gradients along the body affect the stability and growth of the boundary layer, such approximations cannot be used for this body. The pressure distribution along the body was first calculated from potential flow theory¹² and is shown in Fig. 4 as $(p - p_\infty) / (\frac{1}{2}\rho U_\infty^2) = 1 - (U/U_\infty)^2$, where p_∞ is the pressure of the undisturbed stream far ahead, ρ is the fluid density, U is the velocity at the outer edge of the boundary layer, and U_∞ is the free-stream velocity. The contributions from the tow-staff fairing and tail fins have been neglected in this calculation. Table II shows the pressure gradient, $(L/\frac{1}{2}\rho U_\infty^2)(dp/dx)$, at several of the hydrophone locations, nondimensionalized by body length, L , and the stagnation pressure.

The pressure distribution was substituted into the boundary-layer equations for axisymmetric flow.¹³ Transition was found to be possible over a range of values, for instance, from approximately 0.08L–0.43L at 30 kt. For a smooth body with no natural turbulence in the free stream, transition would occur at 0.43L. If the body has some surface roughnesses or if turbulence exists in the free stream, transition could occur as far forward as 0.08L. For the towed body, because of slight surface roughnesses and the natural turbulence

TABLE I. Depth of towed body for different speeds and towing-cable lengths.

Speed (knots)	Cable length (feet)	Depth (feet)
30	175	58
	100	32
25	175	62
	100	37
20	150	60
	100	46
	50	23

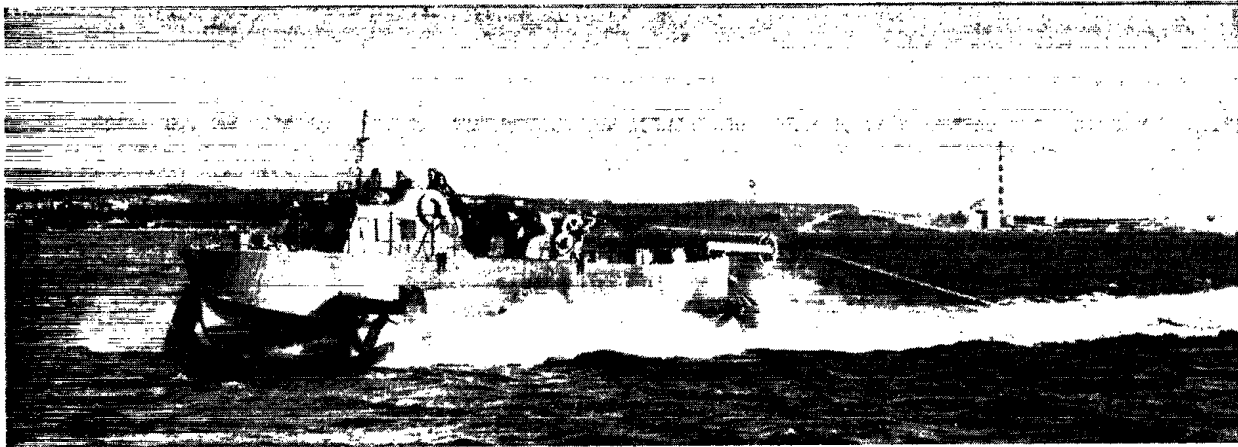


FIG. 3. The hydrofoil craft, *BADDECK*, during towing.

in the water, transition was expected to occur near the calculated forward limit. The approximate location was identified from the noise recorded by hydrophones 4 and 5, which were in this region.

The turbulent boundary-layer-displacement thickness, δ^* , was calculated assuming that transition occurred at some known point. Figure 5 shows δ^* as a function of the axial distance along the body for a towing speed, V , of 30 kt with transition assumed to occur at $0.08L$, that is, between hydrophones 4 and 5. The ratio of the transducer diameter to boundary-layer-displacement thickness, D/δ^* , is also shown in Table II for some of the hydrophones in the turbulent boundary layer.

III. RESULTS AND DISCUSSION

A. Flow Noise

Figure 6 shows the pressure spectral density, $P(f)$, obtained from several of the flush-mounted hydrophones for speeds of 25 and 30 kt at 175-ft towing-cable length. Hydrophones 1, 4, and 5 are in the nose cone, the first at the stagnation point at the nose and the other two at $0.07L$ and $0.10L$, respectively. Hydrophone 7 is in the center section at $0.28L$. The data can be divided into two regimes, above and below 500 Hz, suggesting that different mechanisms may apply in the two regimes. The spectra above 500 Hz will be discussed first.

TABLE II. Pressure gradient and transducer diameter to boundary-layer displacement thickness ratio.

H/P	x/L	$\frac{L}{\frac{1}{2}\rho U^2} \frac{d\phi}{dx}$	D/δ^* (estimated)
3	0.03	-8.5	...
4	0.07	-2.9	...
5	0.10	-2.0	...
6	0.22	-0.8	3.5
7	0.28	-0.6	2.7
8	0.35	-0.4	2.1

Since hydrophone 4 is ahead of the calculated forward limit for the transition point, the boundary layer is presumably laminar at this point. The similarity in the measured noise between hydrophones 5 and 4 at 25 kt indicates that the boundary layer at hydrophone 5 is also very probably laminar. The turbulence generated by the towed body is accompanied by a relatively weak farfield or radiated sound at frequencies below approximately 3 kHz because of the small diameter of the body. The hydrophones in the laminar boundary layer should respond to this component of the flow-noise field. The increase in the spectrum levels with speed is expected because of the increased radiation field. Above 3 kHz, when the diameter of the body exceeds the wavelength of sound, the farfield generation is improved and hydrophone 1 receives approximately as much noise as hydrophones 4 and 5.

The boundary layer at hydrophone 7 is expected to be turbulent. Since the hydrophone has a very small diameter, it will respond to the nearfield flow noise arising from pressure fluctuations in the boundary layer. The nearfield flow-noise spectrum level should be approximately constant for about an octave below a cutoff frequency,¹ $f_0 = U/(5\delta^*) \approx 3$ kHz, and decrease

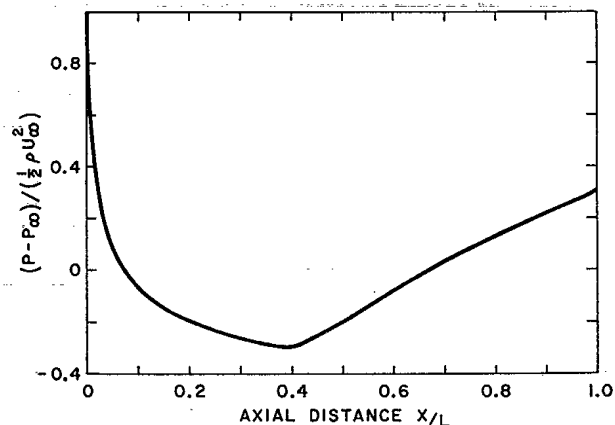


FIG. 4. Nondimensionalized pressure distribution along body from potential flow theory.

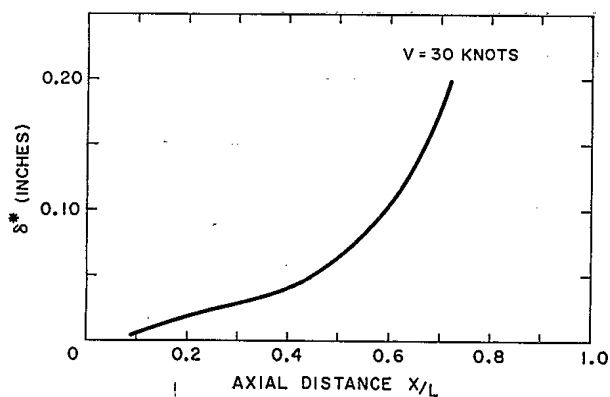


FIG. 5. Calculated boundary-layer thickness at 30-kt towing speed.

as f^{-n} above f_0 . The spectrum obtained from hydrophone 7 illustrates this behavior. The increase in the spectrum level above 3 kHz of approximately 5 to 6 dB, when the velocity increases from 25 to 30 kt, is consistent with the increase expected in the wall pressure spectrum with speed.

Figure 7 shows the pressure spectra in nondimensional form obtained from hydrophones in the turbulent boundary layer, where fD/U is the nondimensional frequency and $P(f)U/\tau_w^2 D$ is the nondimensional spectral density. The velocity, U , is the velocity at

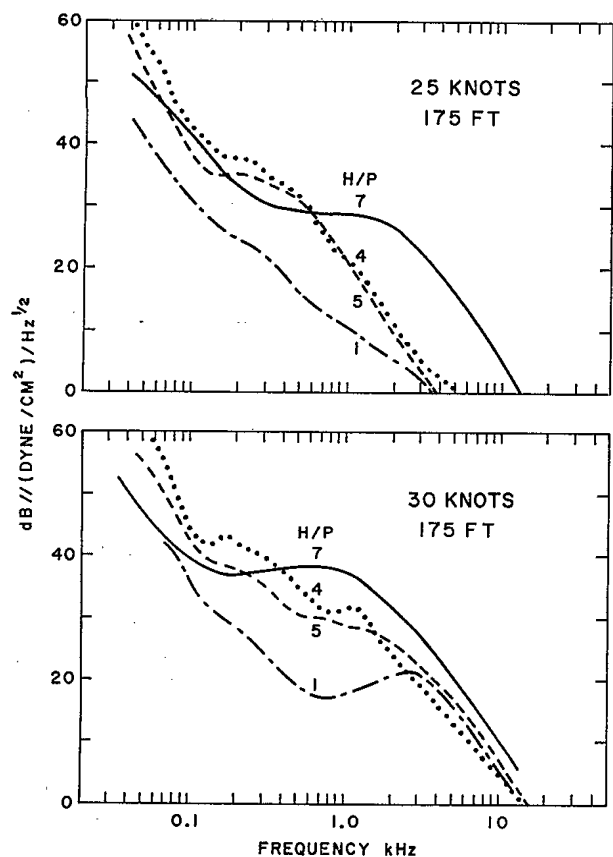


FIG. 6. Pressure spectra from flush-mounted hydrophones for 25 and 30 kt at 175-ft towing-cable length.

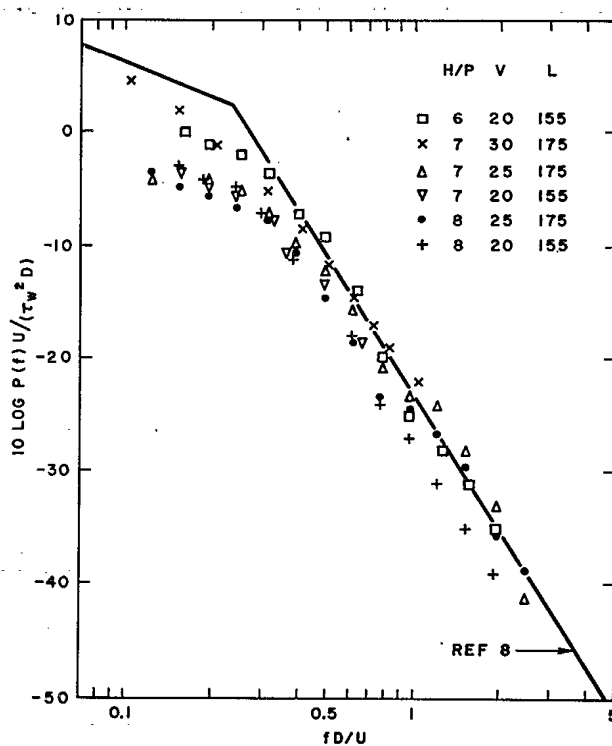


FIG. 7. Nondimensionalized spectra for turbulent-boundary-layer pressure fluctuations (V in knots, L in feet).

the outer edge of the boundary layer at the hydrophone location; D is the hydrophone diameter; and τ_w is the wall shear stress. The effect of the pressure gradient on the shear stress is difficult to calculate, and hence, the shear stress has been obtained from an approximation for a flat plate.¹³

$$\text{SHEAR STRESS} = \tau_w = (0.006361/R_0^{0.1686})\rho U^2,$$

where R_0 is the boundary-layer Reynolds number. Above $fD/U > 0.4$, the spectral density decreases as the fourth power of frequency. Shown for comparison is a solid line based on a large number of measurements obtained by Foxwell⁸ in the turbulent boundary layer around a rotating cylinder.

B. Wall Vibration Noise

Figure 8 shows the effect of speed and cable length on the pressure and acceleration spectra obtained from a flush-mounted hydrophone-accelerometer pair on the nose cone (hydrophone and accelerometer 3 at $0.03 L$), where the boundary layer is laminar. For constant cable length, the pressure and acceleration spectra for frequencies above 500 Hz increase with increasing towing speed. For constant towing speed, the pressure and acceleration spectra increase with decreasing cable length.

The similarity between the pressure and acceleration spectra for the various towing conditions indicates that the body-wall vibrations have an effect on the measured pressure level in the laminar boundary layer. If the

NOISE ON AN UNDERWATER TOWED BODY

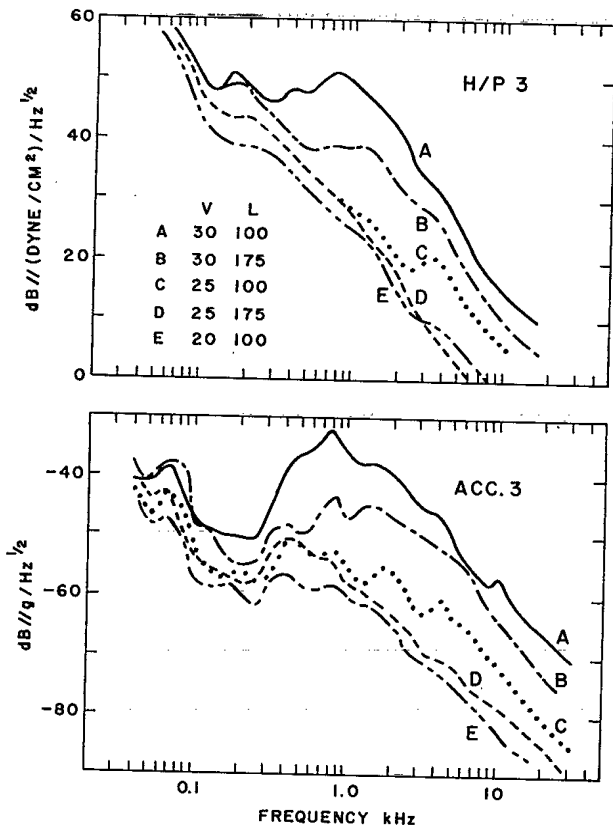


FIG. 8. Pressure and acceleration spectra from flush-mounted hydrophone 3 and accelerometer 3 in laminar boundary layer (V in knots, L in feet).

Wall vibrations are assumed to give rise to plane waves only, the vibration level can be converted to a pressure level, ρcv , where ρ is the density of water, c is the velocity of sound, and v is the particle velocity

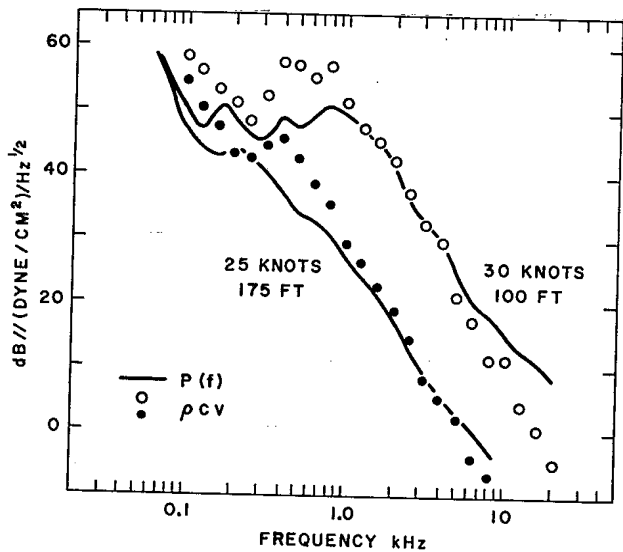


FIG. 9. Comparison between measured pressure from hydrophone 3 and wall vibration pressure (ρcv) from accelerometer 3 in laminar boundary layer at 30 kt with 100-ft towing-cable length, and at 25 kt with 175-ft towing-cable length.

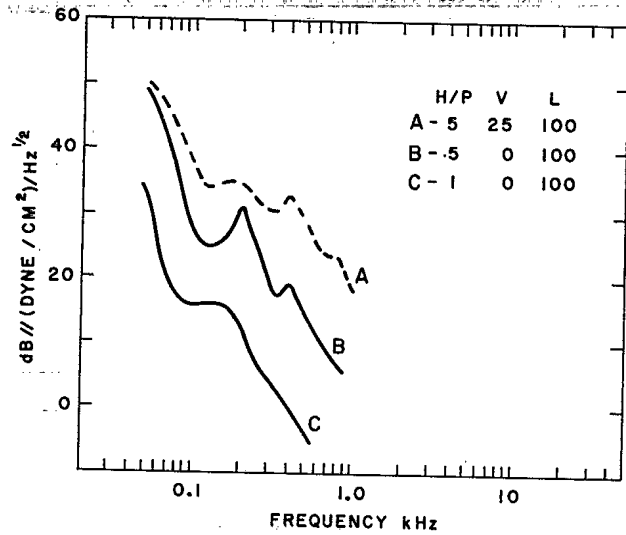


FIG. 10. Comparison between manual excitation of towing cable and towing at 25 kt (100-ft cable length).

at the surface of the wall. The particle velocity can be obtained from the accelerometer readings. Figure 9 shows a comparison between the pressure level computed from accelerometer 3 using ρcv and the actual measured pressure from hydrophone 3 for speeds of 30 kt at 100-ft cable and 25 kt at 175-ft cable. The agreement above 1 kHz indicates that the measured pressure level is due to wall vibrations. At low frequencies, the plane-wave approximation used to calculate the pressure is not expected to hold, because of the curvature of the body, and the measured and computed values do not agree.

Under the turbulent boundary layer, accelerometer readings show that the acceleration spectra are similar to those shown in Fig. 8. For most towing conditions, the flush-mounted hydrophones in the turbulent boundary layer record the nearfield flow noise. However, at

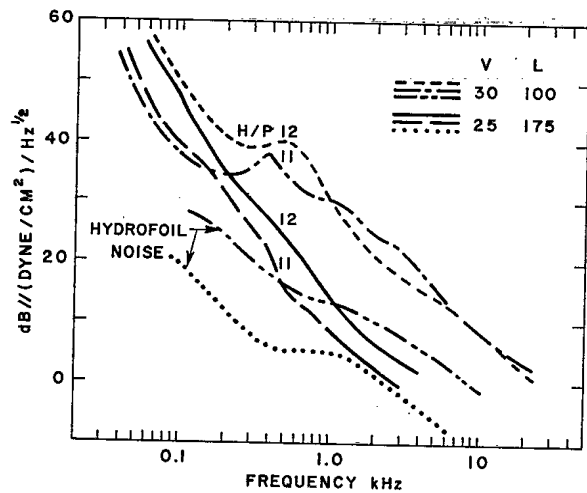


FIG. 11. Radiated noise spectra inside body aft of tow point (hydrophone 11) and inside nose cone (hydrophone 12) obtained with cylindrical hydrophones compared to hydrofoil radiated noise.

30 kt and 100-ft towing-cable length, the nearfield flow noise is masked and the measured pressure level is probably due to increased wall vibrations.

Wall vibrations can arise from the turbulent flow about the body, by vortices shed by the tail fins, and from cable vibrations. An additional source of noise and vibration when the cable length is shortened at high speed may be cavitation. For instance, at 30 kt and 100-ft towing-cable length, the body is only 32 ft deep (Table I), and cavitation is certainly possible at locations such as the tow point. Skudrzyk and Haddle report that the vibration and noise level may increase by as much as 20 dB when cavitation is present.⁵

The increase at frequencies below 500 Hz in both the pressure and acceleration spectra is most likely due to cable vibrations and eddies that separate from the cable and tail and excite the body like a loudspeaker membrane. During the towing trials, fluctuations in the cable tension were observed at the towing craft. Figure 10 shows the pressure spectrum levels obtained on hydrophones 1 and 5 by suspending the body in water with 100 ft of cable and manually shaking the cable. For comparison, the pressure spectrum obtained on hydrophone 5 at 25-kt towing speed and 100-ft cable is also shown. The similarity of the results for hydrophone 5 indicates that cable vibrations, which are transmitted to the body wall, are the cause of the high spectrum levels observed in this frequency range. The vibrations of the cable may originate at the towing craft itself, at the air-water interface, and from the drag of the cable through the water.

C. Radiated Noise

The radiated noise inside the water-filled body was measured with $\frac{1}{2}$ -in. cylindrical hydrophones. Figure 11 shows pressure spectra obtained from hydrophone 12 located in the middle of the nose cone, and hydrophone 11 located just aft of the tow point. At high frequencies, these hydrophones respond to the same farfield radiated noise field as the flush-mounted hydrophones in the laminar boundary layer. At frequencies below 5 kHz, the spectrum levels measured within the body are lower than those measured with the flush-mounted hydrophones.

Also shown in Fig. 11 is the hydrofoil's radiated noise for 25 kt at 175-ft distance and 30 kt at 100-ft distance. At 25 kt, the radiated noise above 2 kHz measured with hydrophone 11 is similar to that expected from the hydrofoil. At 30 kt, the increase in noise within the body is approximately 10 dB greater than the increase in the radiated noise of the hydrofoil. The slope of -6 dB/oct at this speed seems consistent with the spectrum of cavitation noise.

IV. SUMMARY

The results of noise measurements on a hydrofoil-towed body of revolution show that noise is caused by

body-wall vibrations, pressure fluctuations in the turbulent boundary layer, and farfield radiated noise sources. In the turbulent boundary layer, pressure fluctuations are recorded with flush-mounted hydrophones at frequencies above 1 kHz. In the laminar boundary layer, the noise observed with flush-mounted hydrophones is caused by wall vibrations and radiated noise sources. Possible sources of wall vibrations are cable vibrations, tail-fin vibrations, turbulent flow downstream from the transition point, and cavitation. Measurements of the radiated noise inside the body suggest that, at high frequencies and low velocities, the radiated noise of the hydrofoil is important, whereas at low frequencies or high velocities, other sources of noise are important.

ACKNOWLEDGMENT

The authors wish to thank Dr. E. J. Skudrzyk of the Ordnance Research Laboratory of the Pennsylvania State University for his helpful comments in preparing this paper.

* Present address: SACLANT ASW Research Center, Viale, San Bartolomeo 400, La Spezia 19026, Italy.

† Present address: Norweg. Def. Res. Estab, Karl Johansvern, Horten, Norway.

¹ E. J. Skudrzyk and G. P. Haddle, "Noise Production in Turbulent Boundary Layers by Smooth and Rough Surfaces," *J. Acoust. Soc. Amer.* 32, 19-34 (1960).

² W. W. Willmarth and C. E. Wooldridge, "Measurements of the Fluctuating Pressure at the Wall Beneath a Thick Turbulent Boundary Layer," *J. Fluid Mech.* 14, Pt. 2, 187-210 (1962).

³ George F. Carey, John E. Chlupsa, and Howard H. Schloemer, "Acoustic Turbulent Water-Flow Tunnel," *J. Acoust. Soc. Amer.* 41, 373-379 (1967).

⁴ H. H. Schloemer, "Effect of Pressure Gradients on Turbulent Boundary Layer Wall Pressure Fluctuations," *J. Acoust. Soc. Amer.* 42, 93-113 (1967).

⁵ E. J. Skudrzyk and G. P. Haddle, "Flow Noise," *Ordnance Res. Lab., Penn. State Univ.* (25 Oct. 1960).

⁶ C. R. Nisewanger and F. B. Sperling, "Flow Noise Inside Boundary Layers of Buoyancy-Propelled Bodies," *U. S. Naval Ord. Test Station Tech. Publ.* 3511, NAVWEPS Rep. 8519 (April 1965).

⁷ Henry P. Bakewell, Jr., "Turbulent Wall-Pressure Fluctuations on a Body of Revolution," *J. Acoust. Soc. Amer.* 43, 1358-1363 (1968).

⁸ J. H. Foxwell, "The Wall Pressure Spectrum Under a Turbulent Boundary Layer," *Admiralty Underwater Weapons Estab. Tech. Note* 218/66 (August 1966).

⁹ G. P. Haddle and E. J. Skudrzyk, "The Physics of Flow Noise," *J. Acoust. Soc. Amer.* 46, 130-157 (1969).

¹⁰ W. A. Strawderman and R. S. Brand, "Turbulent-Flow-Excited Vibration of a Simply Supported, Rectangular Flat Plate," *J. Acoust. Soc. Amer.* 45, 177-192 (1969).

¹¹ R. B. Gilchrist and W. A. Strawderman, "Experimental Hydrophone Size Correction Factor for Boundary Layer Pressure Fluctuations," *J. Acoust. Soc. Amer.* 38, 298-302 (1965).

¹² L. Landweber, "The Axially Symmetric Potential Flow About Elongated Bodies of Revolution," *David Taylor Model Basin Rep.* 761 (August 1951).

¹³ P. S. Granville, "The Calculation of the Viscous Drag of Bodies of Revolution," *David Taylor Model Basin Rep.* 849 (July 1953).

8903
71-02588